EE568 – Selected Topics on Electrical Machines

Project #4: PM Motor Comparison Analysis

by

Hakan Saraç - 2408086

Table of Content

1 Introduction

In this project, an Interior Permanent Magnet (IPM) machine is designed analytically. Before starting with the calculations, first a literature review is provided, in which different types of IPM machines are investigated. After that, the analytical calculations are provided.

2 Literature Review

For EV and HEV applications, there are quite design challenges. Such applications require small volume, high efficiency, high power over a wide speed range. Considering these requirements, induction machines and permanent magnet machines have been widely investigated in the literature. Due to their better power factor, higher torque density, better efficiency characteristics, permanent magnet machines are the preferred choice for the vehicle applications.

In the permanent magnet class, Interior Permanent Magnet (IPM) machines are superior to the Surface Permanent Magnet (SPM) machines. The reason is that the IPM machine have reaction and reluctance torque while SPM machines only have reaction torque component. This lead IPM machines to be more power and torque dense.

IPM machines are being used by various EVs and HEVs, some examples are Toyota Prius, Nissan Leaf and Chevrolet Volt [1]. Although its stator configuration is similar to the other types of machines, the IPM machines can have various rotor designs, each leading to a different performance characteristics [1].

Flux weakening is an important measure in IPMs that are used in electrical vehicle operations, due to the wide torque speed region requirements, and therefore deeply investigated. The torque expression for an IPM machine is given in (1).

$$T_e = 1.5 \cdot p \cdot [\Psi_q \cdot i_q + (L_d - L_q) \cdot i_d \cdot i_q] \quad (1)$$

Since for an IPM machine $L_d < L_q$, reluctance torque can be generated by applying a negative i_d current, which is commonly used for IPM machines. Applying a negative i_d current causes a worse power factor for the machine, which reduces the efficiency of the machine. Moreover, if not acted carefully, the magnets may get demagnetized if applied excessive i_d current.

To overcome this problem, a different IPM machine is investigated in [2], whose rotor structure is given in Figure 1. The proposed machine, called Flux-Intensifying IPM (FI-IPM). A FI-IPM has flux barrier across the q axis, therefore the d axis inductance of this machine is larger than q axis inductance, i.e. $L_d > L_q$. Thus, to generate reluctance torque, a positive i_d current is required. In the flux-weakening region still a negative i_d is required. Nevertheless, FI-IPM machine can have reduced i_d current (and less coercive force on the magnets) for the same operating point [2]. Permanent magnet operating points of a FI-IPM is given in Figure 2.

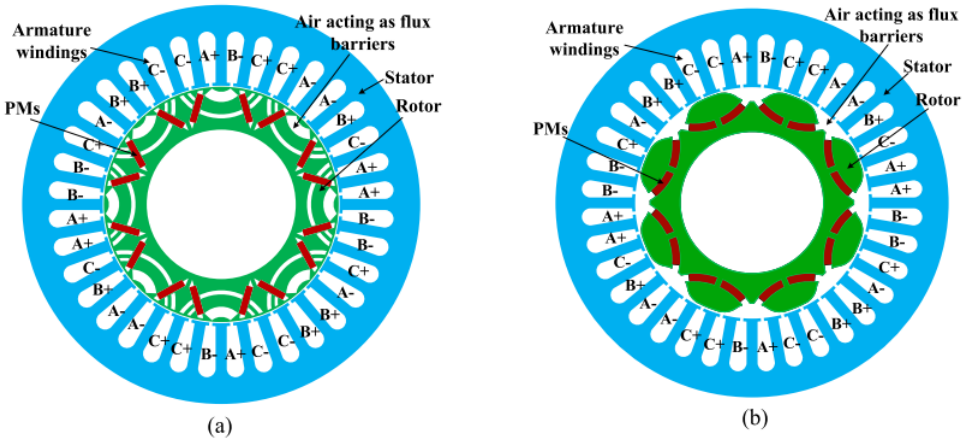

Figure 1: Different FI-IPM machines [2]

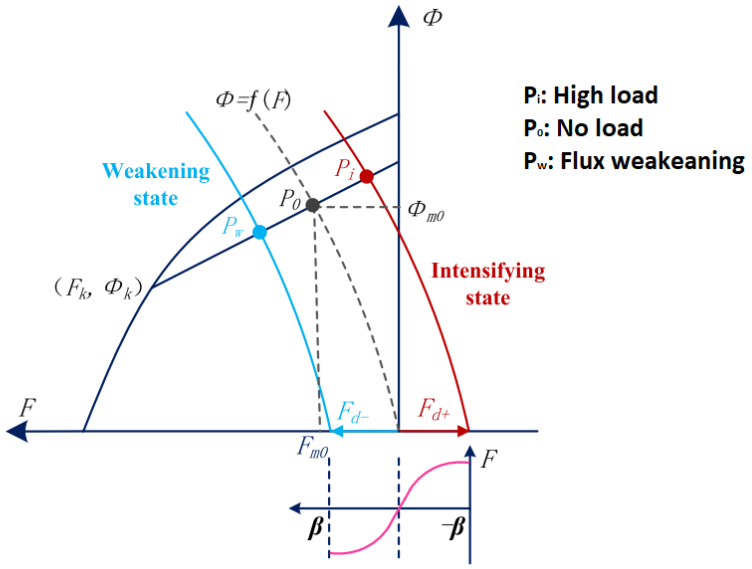

Figure 2: Permanent magnet operating points for an FI-IPM [2]

In [3], different types of rotor designs are compared over a base rotor structure, which are given in Figure 3. These rotor shapes are different in flux barrier shapes. Torque characteristics of those machines are provided in Table 1 [3].

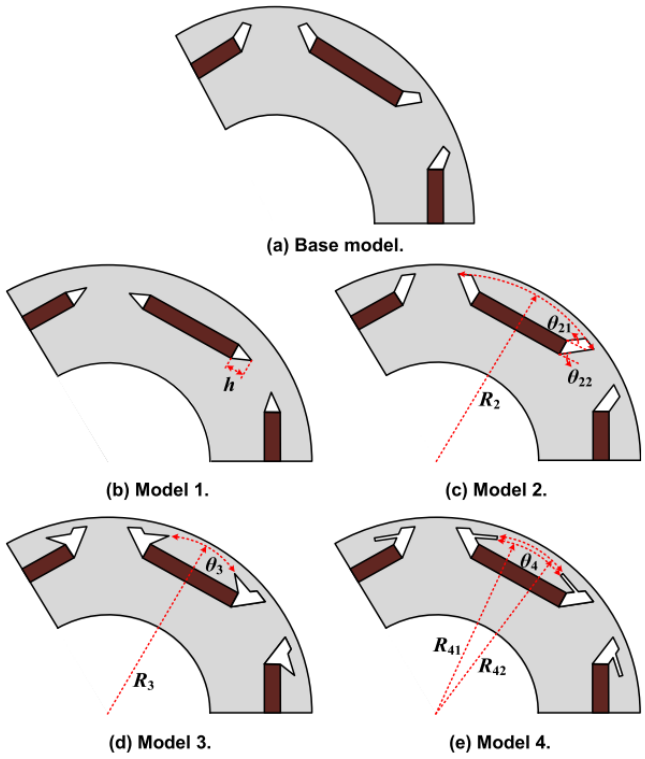

Figure 3: IPM rotor shapes with flux different barriers [3]

Table 1: Torque characteristics of the machines in Figure 3

	Average torque [Nm]	Torque ripple [%]	Cogging torque [Nm]
Base model	206.14	13.4	8.49
Model 1	206.49	7.23	1.16
Model 2	218.23	12.5	5.88
Model 3	223.12	6.47	2.87
Model 4	220.25	8.92	1.58

While designing the rotor shape, the mechanical aspects should also be considered. The pressure and centrifugal forces acting on the rotor may cause permanent magnets to crack or loosen and fly off, irreversibly damaging the machine.

Vibration is also an important problem. It may not cause immediate damage, but the lifetime of the machine may reduce. Therefore, the vibrations should also be considered as in [4].

U-shaped, V-shaped and conventional shape rotor schemes are compared in [5]. For the stated ratings, it is found that the V-shaped rotor have better performance for the specified ratings.

3 Specifications of the machine

The machine will be designed for an electrical vehicle application. The size limits and voltage, current and power ratings of the machine are as follows.

- Type: Interior Permanent Magnet Synchronous Machine
- Three phase, 125kW, 350 $V_{linetoline\text{-}rms}$, 210 A_{rms}
- Torque density 2.5Nm/kg, Power density 1.25kW/kg
- 150kg maximum mass
- Outer diameter < 350mm
- Stack length < 250mm

4 Analytical Calculations

4.1 Initial Design

At first, the fundamental specifications of the machine are chosen. These parameters are listed on Table 2. The number of slots is decided so that each slot have around 10mm opening.

Table 2: Fundamental specifications of the machine

NumberOfPoles	12
B_{airgap_peak}	0.8 T
NumberOfSlots	54
NumberOfPhases	3
FillFactor	0.8
Di	180mm
$D_{slotend}$	300mm
Do	350mm
Length	250mm

4.2 Winding Design

The number of slots per pole per phase is 1.5 which makes it a fractional slot winding machine. The electrical angle between each coil is given in (2). Resulting winding distribution and vectorial distribution of induced slot voltages are given in Table 3, Figure 4 respectively.

$$CoilsPhaseShift = 360° * \frac{\frac{12}{2}}{54} = 40° \quad (2)$$

Table 3: Winding distribution of the machine

Slot Number	1	2	3	4	5	6	7	8	9
Electrical Angle	0°	40°	80°	120°	160°	200°	240°	280°	320°
Coil distribution	A1	A1	-C1	B1	B1	-A1	C1	C1	-B1
	A1	-C1	-C1	B1	-A1	-A1	C1	-B1	-B1
Slot Number	10	11	12	13	14	15	16	17	18
Electrical Angle	0°	40°	80°	120°	160°	200°	240°	280°	320°
Coil distribution	A2	A2	-C2	B2	B2	-A2	C2	C2	-B2
	A2	-C2	-C2	B2	-A2	-A2	C2	-B2	-B2

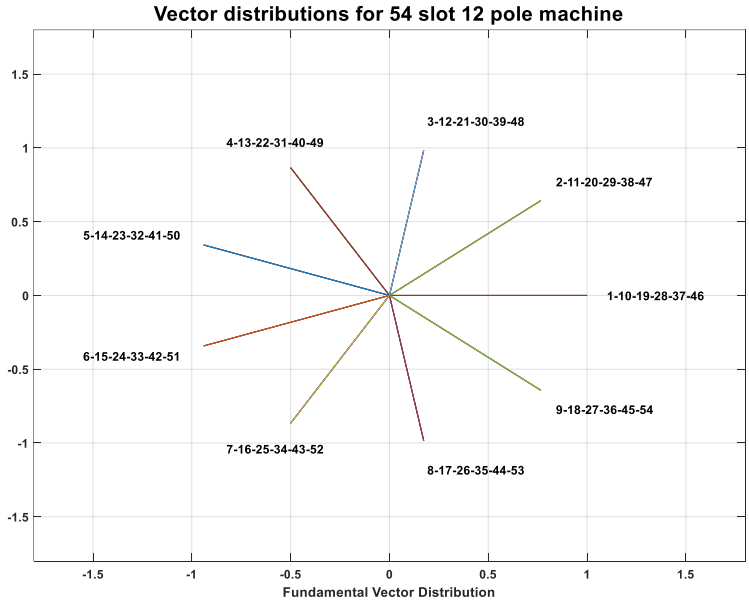

Figure 4: Vectorial Representation of Induced Phase Voltages

The distribution factor, the pitch factor and winding factor values are provided in (3),(4) and (5) respectively.

$$k_d = \frac{Vectorial\ Sum}{Scalar\ Sum} = 0.9466 \tag{3}$$

$$k_p = sin(\frac{MeanAngleBetweenCoils}{2}) = sin(\frac{173.333}{2}) = 0.9983 \tag{4}$$

$$k_w = k_d k_p = 0.945 \tag{5}$$

4.3 Machine Dimensions

Using the dimensions stated in Table 2, the slot area and copper are is calculated in (6), (7), (8), (9), (10), (11). The teeth are chosen to have parallel edges.

$$SlotHeight = \frac{D_{SlotEnd} - D_i}{2} = 60mm \tag{6}$$

$$SlotWidthInner = \frac{\pi D_i}{2 * NumberOfSlots} = 5.2mm \tag{7}$$

$$SlotWidthOuter = \frac{\pi D_{SlotEnd}}{2 * NumberOfSlots} = 8.7mm \tag{8}$$

$$\text{SlotArea} = \frac{\text{SlotWidthInner} + \text{SlotWidthOuter}}{2} * \text{SlotHeight} = 4.1888 * 10^{-4}\ \text{m} \tag{9}$$

$$\text{ToothArea} = \text{SlotHeight} * \text{SlotWidthInner} = 3.1416 * 10^{-4}\ \text{m} \tag{10}$$

$$\text{BackCoreThickness} = \frac{D_o - D_{SlotEnd}}{2} = 25mm \tag{11}$$

4.4 Electrical and Magnetic Specifications

For an electrical vehicle application, the size of the machine is critical. Therefore, to be able to make a machine smaller, liquid cooling is necessary. The liquid cooling provides us to choose a higher electrical loading value. Liquid cooling enables to choose higher current density values. The current density is chosen as **12 A/mm²**. Since the maximum RMS current of the machine is **210 A**, the resultant copper area is given in (12).

$$CopperArea = \frac{210\ A}{12\ A/mm^2} = 17.5mm2 \tag{12}$$

This copper area value corresponds to AWG5 wire, which has **4.621mm** diameter and has **16.7 mm²**. Using the fill factor value, number of turns are given in (13).

$$NumberOfTurns = \frac{\text{SlotArea} * \text{FillFactor}}{WireArea} \approx 20 \tag{13}$$

$$FluxPerPole = \frac{B_{airgap\_peak}\pi D_i \text{StackLength}}{NumberOfPoles} = 9.4\ mWeber \tag{14}$$

The back-core flux density value is calculated in (15), which is an acceptable value for a water-cooled machine.

$$BackCoreFluxDensity = \frac{FluxPerPole}{BackCoreThickness * StackLength * 2} = 0.75\ Tesla \tag{15}$$

Electrical loading value is calculated in (16). To prevent overheating, the peak RMS per coil group needed to be reduced. To achieve that, the windings of the machine will be connected in parallel. This way, the electrical loading of the machine will be more reasonable for a liquid cooled machine.

$$A_{RMS} = \frac{\text{N}_{\text{turn}} * I_{RMS-max} * N_{slots}}{\pi * D_i * 2} = 200535.23\ A/m \tag{16}$$

The machine constant is provided in (17).

$$C = \frac{\pi^2 k_w A_{RMS} B_{airgap\_peak}}{\sqrt{2}} = 1.058 * 10^6 \tag{17}$$

The coils span is around **5 slots**. Therefore, approximate phase resistance is calculated in (18) and (19) respectively.

$$\text{LengthPerTurn} = 2 * \text{StackLength} + 2 * \text{SpanLength} = 0.6\text{m} \tag{18}$$

$$\begin{aligned}\text{ResistancePerPhase} &= 1.68 * 10^{-8} \frac{\text{LengthPerTurn}}{\text{CopperAreaPerCoil}} * \frac{NumberOfTurns}{NumberOfParallelWindings} \\ &= 6m\Omega\end{aligned} \tag{19}$$

5 References

[1] Y. Yang *et al.*, “Design and Comparison of Interior Permanent Magnet Motor Topologies for Traction Applications,” *IEEE Trans. Transp. Electrif.*, vol. 3, no. 1, pp. 86–97, 2017.

[2] X. Zhu, W. Wu, S. Yang, Z. Xiang, and L. Quan, “Comparative design and analysis of new type of flux-intensifying interior permanent magnet motors with different Q-axis rotor flux barriers,” *IEEE Trans. Energy Convers.*, vol. 33, no. 4, pp. 2260–2269, 2018.

[3] E. Sayed, Y. Yang, B. Bilgin, M. H. Bakr, and A. Emadi, “A comprehensive review of flux barriers in interior permanent magnet synchronous machines,” *IEEE Access*, vol. 7, pp. 149168–149181, 2019.

[4] D. W. Kang, “Analysis of Vibration and Performance Considering Demagnetization Phenomenon of the Interior Permanent Magnet Motor,” *IEEE Trans. Magn.*, vol. 53, no. 11, pp. 10–16, 2017.

[5] Y. Zhang, W. Cao, S. McLoone, and J. Morrow, “Design and Flux-Weakening Control of an Interior Permanent Magnet Synchronous Motor for Electric Vehicles,” *IEEE Trans. Appl. Supercond.*, vol. 26, no. 7, 2016.